

## Distribution of Mouse Adenovirus Type 1 in Intraperitoneally and Intranasally Infected Adult Outbred Mice

ADRIANA E. KAJON,<sup>1</sup> CORRIE C. BROWN,<sup>2</sup> AND KATHERINE R. SPINDLER<sup>1\*</sup>

*Department of Genetics, Franklin College of Arts and Sciences,<sup>1</sup> and Department of Veterinary Pathology, College of Veterinary Medicine,<sup>2</sup> University of Georgia, Athens, Georgia*

Received 2 September 1997/Accepted 14 October 1997

**In situ nucleic acid hybridization and immunohistochemistry were used to determine the histological localization of mouse adenovirus type 1 (MAV-1) during acute infection of adult mice infected either intraperitoneally or intranasally with 1,000 PFU of wild-type virus. Organ samples were collected from days 1 to 17 postinfection for the intraperitoneally infected mice and from days 1 to 13 for the intranasally infected mice. Endothelial cells of the brain and spinal cord showed extensive evidence of MAV-1 infection. Endothelial cells in lungs, kidneys, and other organs were also positive for MAV-1, indicating a widespread involvement of the systemic circulation. The presence of viral nucleic acid and/or antigen was also demonstrated in lymphoid tissue. The spleens, Peyer's patches, and peripheral lymph nodes showed positive staining at various times postinfection in mice infected by either route. Virus-infected cells in the spleen exhibited a stellate shape and were localized to the red pulp and germinal centers, suggesting that they are cells of the mononuclear phagocytic system.**

Mouse adenovirus type 1 (MAV-1), first isolated by Hartley and Rowe in 1960 (11), is the best characterized of the two known serotypes of adenovirus that infect the house mouse. MAV-1 infection of laboratory mice provides an ideal model system for the study of adenoviral pathogenesis and virus-host interactions in vivo. The experimental infection of adult and newborn mice has been studied by several groups. MAV-1 has been shown to establish a systemic infection involving the spleen, heart, adrenals, intestine, lung, liver, kidney, brain, and spinal cord (20). Whereas inoculation of suckling mice at low doses usually results in fatal disease, among adult immunocompetent mice, mortality is low and a subclinical persistent infection with a prolonged viremia is established (24, 25). However, inoculation of adults with high doses of MAV-1 results in clinical disease and death (10, 18, 26). Although reports are inconsistent, signs associated with MAV-1 infection usually include ruffled coat, hunched posture, lethargy, and a wasting disease. Clinical and pathologic evidence of central nervous system compromise following intraperitoneal (i.p.) infection has also been recently reported (10, 18).

Despite a number of studies of experimental MAV-1 infection of mice, the precise identity of the cell types that support MAV-1 replication during acute infection and the major site of virus persistence are still unclear. A tropism for endothelial cells was noted in several studies examining MAV-1-induced pathology in the adrenal glands, respiratory tract, and heart valves (4, 5, 12, 13, 26). Other cell types described as harboring virus include Purkinje cells of the cerebellum, adrenal parenchymal cells, fibroblasts of heart valves, and myocytes of myocardium (4, 5, 13, 24). Leukocyte-associated viremia has been demonstrated, although the infected cell types were not identified (24). As suggested by the prolonged urinary excretion of infectious virus (24, 25) and the detection of viral intranuclear inclusion bodies in tubular epithelial cells up to 70 days postinfection (dpi) (7), the kidney may be a site of persistence.

With the aim of achieving a more detailed definition of

MAV-1 tropism in the natural host, in situ hybridization and immunohistochemistry were used to investigate viral infection of organs previously shown to support replication during the course of in vivo infection. Our results indicate that the vascular endothelium and lymphoid tissue are major sites of infection and replication in acutely infected mice.

### MATERIALS AND METHODS

**Mice.** Four-week-old NIH Swiss outbred mice were purchased from Harlan Sprague Dawley, Inc., and used for experimental infection within 1 week of arrival. Animals were kept in microisolator cages in groups of two to four individuals and allowed access to food and water ad libitum.

**Experimental infections.** Mice were inoculated either intraperitoneally (i.p.) ( $n = 19$ ) or intranasally (i.n.) ( $n = 20$ ) with  $10^3$  PFU of our standard wild-type strain of MAV-1 (2). Control mice were inoculated with an equivalent volume of conditioned cell culture medium. One mouse served as a control for the i.p. infection, and two mice served as controls for the i.n. infection. Organ samples were collected at days 1, 3, 5, 7, 9, 11, 13, and 17 postinfection (p.i.) for the i.p.-infected mice and at days 1, 2, 3, 4, 5, 7, 9, 11, and 13 p.i. for the i.n.-infected mice. Animals were euthanized by inhalation of  $\text{CO}_2$  and bled from the heart immediately postmortem and just prior to necropsy.

**Histopathology.** The following organs were harvested and fixed in 10% formalin: spleen, lung, heart, small and large intestine, prefemoral and mandibular lymph nodes, liver, kidney, heart, brain, and spinal cord (the latter only in i.n.-infected mice). After 24 h in formalin, tissues were embedded in paraffin. In a few cases where embedding was delayed, tissues were transferred from formalin to phosphate-buffered saline after 24 h of fixation. Once embedded in paraffin, 3- $\mu\text{m}$  sections were cut for histopathology, in situ hybridization, and immunohistochemistry. For histopathology, sections were stained routinely with hematoxylin and eosin.

**In situ hybridization.** An antisense digoxigenin riboprobe was prepared by transcribing a segment of the E3 region from a class 1 cDNA inserted into pBluescript SK- vector (3). The resulting labeled product was 714 nucleotides in length. The transcript concentration was determined by dot blot comparison with a known standard digoxigenin-labeled RNA. Paraffin sections were deparaffinized, rehydrated, and digested with proteinase K (5  $\mu\text{g}/\text{ml}$ ) for 15 min at 37°C. Approximately 25 ng of probe was used per slide. Hybridization occurred overnight at 52°C in a solution consisting of 50% formamide, 5 $\times$  SSC (1 $\times$  SSC is 0.15 M NaCl plus 0.015 M sodium citrate), 5% blocking reagent (Boehringer Mannheim, Indianapolis, Ind.), 1% *N*-lauroylsarcosine, and 0.02% sodium dodecyl sulfate (SDS). The following day, stringent washes were done at 55°C and room temperature with decreasing concentrations of SSC and SDS. Slides were then incubated with anti-digoxigenin-alkaline phosphatase (Boehringer Mannheim) for 2 h at 37°C. The substrate was nitroblue tetrazolium and 5-bromo-4-chloro-3-indolylphosphate (Boehringer Mannheim). Color development progressed for 1 to 3 h. Slides were counterstained lightly with hematoxylin and coverslipped with Permount for a permanent record.

**Immunohistochemistry.** Sections were deparaffinized, rehydrated, and digested with 0.01% trypsin for 20 min at 37°C. After blocking, sections were

\* Corresponding author. Mailing address: Department of Genetics, University of Georgia, Life Sciences Bldg., Athens, GA 30602-7223. Phone: (706) 542-8395. Fax: (706) 542-3910. E-mail: spindler@uga.cc.uga.edu.

incubated at 37°C for 2 h with a primary antiserum to viral structural proteins (AKO-1-68, a rabbit polyclonal antiserum to MAV-1 purified virions [see below]), factor VIII-related antigen (polyclonal antibody 016P; Bio Genex, San Ramon, Calif.), or T cell-CD3 antigen (DAKO A/S, Glostrup, Denmark). The AKO-1-68 antivirion antiserum was prepared as follows. Virions were purified by CsCl centrifugation (2), dialyzed against 4 M urea in TE buffer (10 mM Tris [pH 8.0], 1 mM EDTA) for 20 min, and then dialyzed against TE buffer overnight. Protein concentration was determined by the Bradford assay (Bio-Rad). The sample was adjusted to 0.1% SDS, dialyzed against 8 M urea for 1 h, and then dialyzed against phosphate-buffered saline overnight. Doses of 80 µg were used to immunize rabbits, and subsequent boosts were 40 µg. Serum was adsorbed with an acetone powder of 3T6 cells and mouse mononuclear blood cells.

Incubation of tissue sections with biotinylated secondary anti-rabbit antibody (Vector Laboratories, Burlingame, Calif.) was followed by avidin-peroxidase or avidin-alkaline phosphatase (Vector Laboratories). The substrate was diaminobenzidine for peroxidase and Vector Red (Vector Laboratories) for alkaline phosphatase. Sections were counterstained lightly with hematoxylin and coverslipped with Permount for a permanent record.

## RESULTS

**Clinical disease.** In the group inoculated i.p., signs of disease were recorded in three mice as early as day 5 p.i. in the form of hunched posture, ruffled coat, and lethargy. Paralysis was noted in two individuals at days 7 and 8 p.i. One of these two mice was not available for histopathological studies. Among the i.n.-infected mice, overt signs of disease (hunched posture and ruffled fur) were recorded in only one individual, at 5 dpi.

**Gross pathology and histopathology.** Two of the mice i.p.-inoculated and sacrificed at days 3 and 7 p.i. had enlarged spleens. No other gross pathological signs were seen in the i.p.-inoculated mice or in any i.n.-infected mice. Histologically, there was a surprising lack of observable lesions, and inflammatory infiltrates were minimal to nonexistent. Many of the mice had multifocal intra-alveolar hemorrhage without any accompanying inflammatory changes; these hemorrhages were attributable to the method of euthanasia. In the i.p.-infected mice, there was a modest karyorrhexis in lymphoid areas of the spleen at 9 dpi and numerous and prominent germinal centers in the spleen by 13 dpi. In the brain, there was acute degeneration of groups of neurons at 5 and 7 dpi and a focus of gliosis in the cerebellum in one mouse at 13 dpi. Minor foci of microhemorrhages were also observed in the hematoxylin-eosin-stained sections. Rare intranuclear inclusion bodies were noted in capillaries of lung (one mouse at 7 dpi) and small intestine (one mouse at 7 dpi). In the i.n.-infected mice, germinal center formation was noted in the spleen at 7, 9, 11, and 13 dpi. Mandibular lymph nodes appeared reactive at 9 dpi.

**Immunohistochemistry and in situ hybridization.** No major differences were found between the i.n.- and i.p.-infected mice in tissue distribution or cell tropism of the virus. The most intensely infected organs after infection were the spleen, brain, spinal cord, lung, and kidney.

**Infection of vascular endothelium.** Evidence of MAV-1 DNA and antigens was seen in endothelial cells, particularly in the brain and spinal cord (Fig. 1). Immunohistochemistry with an antibody to factor VIII-related antigen, a specific component of endothelial cells, was used in double-staining experiments to confirm that the nucleic acid detected by in situ hybridization was within vascular endothelium (Fig. 1D). Endothelial cells in the lung, kidney, spleen, liver, and other organs also stained positive for MAV-1, indicating a widespread involvement of the systemic circulation (Fig. 2 and 3A).

**Infection of lymphoid tissue.** The presence of viral nucleic acid and/or antigen was demonstrated by in situ hybridization and immunohistochemistry in the spleens, Peyer's patches, and mandibular and prefemoral lymph nodes in mice infected by either route. Virus-infected cells in the spleen were localized to the red pulp and exhibited a stellate shape strongly suggestive

of macrophages (Fig. 4A and B). Between days 13 and 17 p.i., virus could also be detected in the germinal centers. In Peyer's patches and lymph nodes, infected cells were localized primarily in germinal centers of follicles (Fig. 4C). Spatially, the virus-positive cells were not located in B-cell areas. The occurrence of staining in cytoplasmic processes of large stellate cells suggested that the infected elements might be follicular dendritic cells. By combining in situ hybridization and immunohistochemistry protocols, viral infection was found not to involve the T-cell population (Fig. 4D).

**Infection of epithelium.** Rare staining was found in epithelial cells of the distal tubules of the kidney in one i.n.-infected mouse at 4 dpi. As shown in Fig. 3B, viral nucleic acid was found in the epithelial cells lining the renal pelvis in one i.p.-infected mouse sacrificed at 11 dpi. Viral antigen was not detected in these same sections, as assayed by staining with antivirion antibody.

**Spread of MAV-1 after i.p. and i.n. infection.** The time course of infection differed between routes of inoculation (Table 1). However, in both groups, the first signs of presence of viral nucleic acids were found at 3 dpi in the spleen. In the i.n.-infected mice, viral nucleic acid was also found in the mandibular lymph node at 3 dpi. Subsequently there was an extensive positivity in endothelial cells throughout the body. In the i.p.-infected mice, there was more extensive and widespread involvement of endothelium at 7 dpi. In contrast, in the i.n.-infected mice, this widespread vascular involvement was seen later, at 13 dpi.

## DISCUSSION

The major site of MAV-1 infection and replication in outbred adult mice infected either i.p. or i.n. with 1,000 PFU of virus and studied over a 13- to 17-day period was found to be the vascular endothelium, especially that in the brain and spinal cord. The presence of viral nucleic acids and/or antigens was also demonstrated in endothelial cells of the lung, kidney, liver, and spleen at different time points p.i. The absence of significant staining in the heart and adrenal glands is noteworthy and represents a major difference from findings reported by other authors (4, 5, 13, 24). In our hands, staining in these tissues was strictly circumscribed to endothelium.

MAV-1 nucleic acids and antigens were also detected in lymphoid tissue during the course of acute infection. The identity of MAV-1-positive lymphoid cells was investigated by using immunohistochemistry targeting specific cell types. The spatial distribution and morphology of the stained elements suggest that the cell type harboring MAV-1 in lymphoid tissue is a member of the mononuclear phagocytic system and that the initial replication after infection may take place in these cells. In the case of i.p. infection, there would be a large bed of peritoneal macrophages in which virus could replicate, with subsequent early spread of virus to the spleen. In the i.n.-infected mice, the primary site of replication is unknown, but the presence of large mononuclear cells staining in the mandibular lymph node suggests initial replication in macrophages within lymphoid tissue. It is therefore likely that peripheral blood monocytes or dendritic cell precursors are the primary vehicles for virus dissemination during acute infection. This issue must be further investigated by use of additional cell-typing reagents.

Staining of epithelial cells was noted only in the kidney. Infection of the renal tubular epithelium was detected as early as 4 dpi, suggesting that it is an early event during acute infection. At day 11 p.i., viral nucleic acid was also detected in the epithelium lining the renal pelvis.

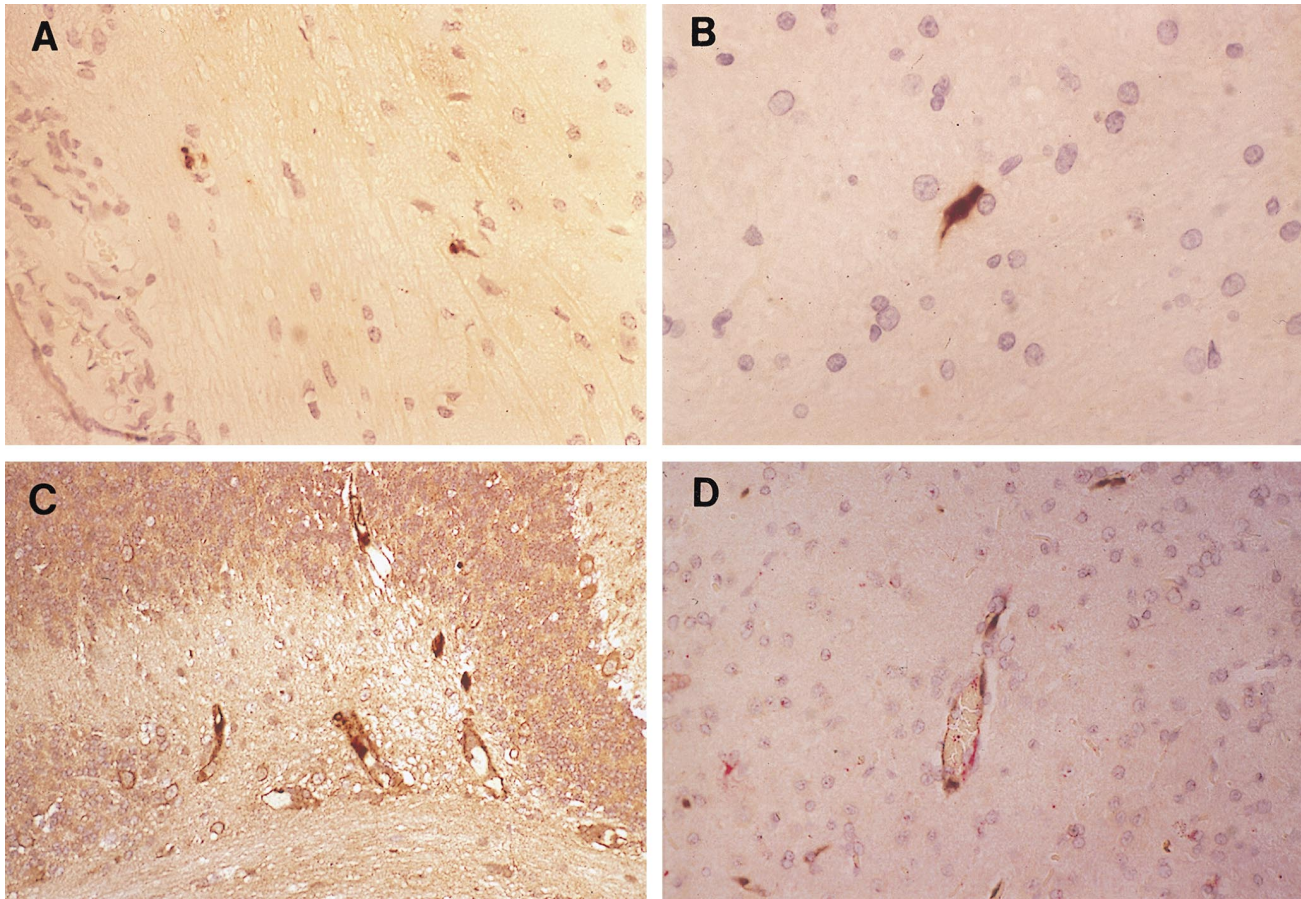


FIG. 1. Infection of vascular endothelium of the central nervous system. (A and B) In situ hybridization with MAV-1 E3 riboprobe. Shown are representative sections of brain (A; magnification,  $\times 145$ ) and spinal cord (B; magnification,  $\times 213$ ) of an i.n.-infected mouse sacrificed at 13 dpi. (C) Immunohistochemistry with antivirion (AKO-1-68) antiserum on a section of brain of an i.p.-infected mouse paralyzed on day 5 p.i. and euthanized at 7 dpi. Magnification,  $\times 116$ . (D) In situ hybridization plus immunohistochemistry with antiserum directed against factor VIII-related antigen on a section of brain of the same mouse as in panel C. Magnification,  $\times 194$ . Sections were counterstained with hematoxylin, photographed on slide film, and digitized on a Nikon Coolscan. Positive viral staining in all panels appears brown; positive factor VIII-related antigen staining in panel D appears red.

The kidney, an immunologically privileged site due to the limited access of cytotoxic T cells to the epithelial surface (1), is the site of persistence of murine K papovavirus, which also behaves as an endotheliotrope during acute infection (8, 9).

Some human adenovirus serotypes of subgenus B:2 have also been shown to be shed in the urine of immunocompromised patients, suggesting that the kidney may be the site of persistence for this particular group as well (19). MAV-1 has been

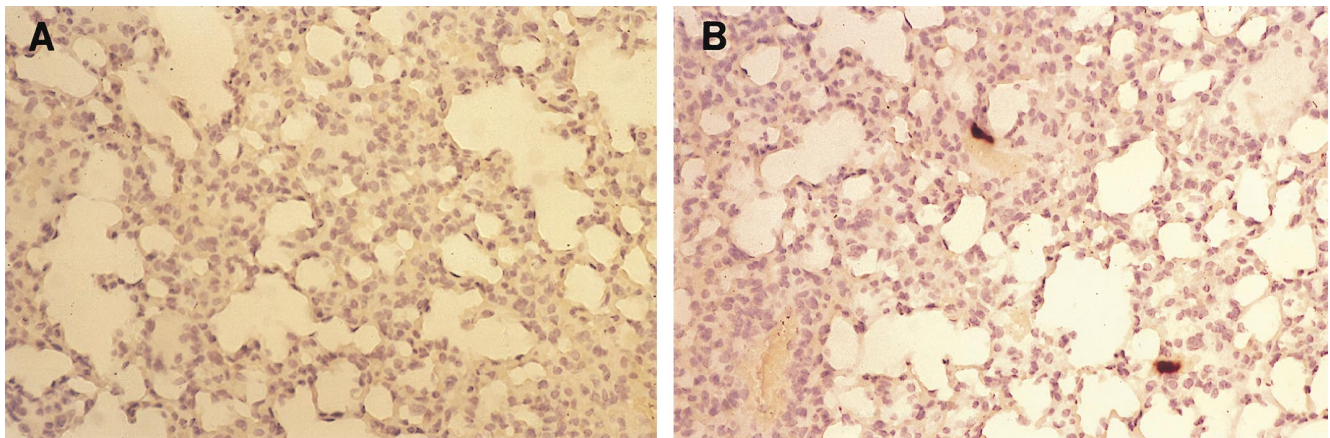


FIG. 2. In situ hybridization with MAV-1 riboprobe of infected vascular endothelium of the lung. (A) Section of lung of a mock-infected mouse; (B) representative section of lung of an i.p.-infected mouse sacrificed at 7 dpi. Magnification,  $\times 97$ .

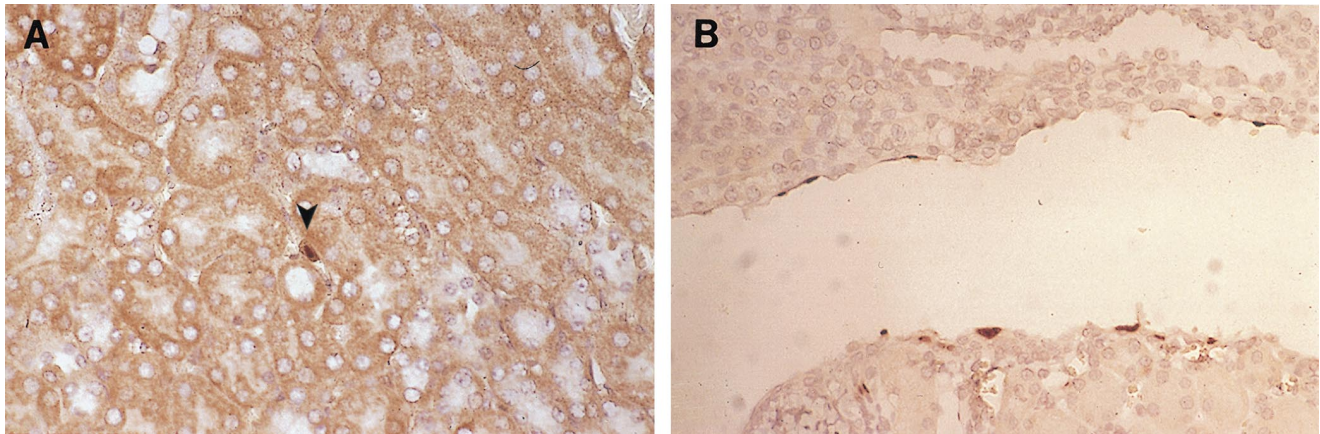


FIG. 3. Infection of the kidney. (A) Endothelial cell staining: immunohistochemistry with antivirion (AKO-1-68) antiserum on a section of kidney of an i.p.-infected mouse sacrificed at 7 dpi. Renal tubuli are seen in cross section with a large stained nuclear inclusion body in the center (arrowhead). Magnification,  $\times 194$ . (B) Staining of epithelial cells lining the renal pelvis: in situ hybridization with MAV-1 E3 riboprobe on a section of kidney of an i.n.-infected mouse sacrificed at 11 dpi. Magnification,  $\times 194$ .

isolated from the urine of infected mice for prolonged periods p.i. (7, 20a). However, the positive specific hybridization for MAV-1 nucleic acids in the absence of immunohistochemical labeling of viral antigens that was obtained in the experiments

described here suggests a nonproductive infection of the renal epithelium at the early stages examined. Similar findings were reported for K-papovavirus infection of newborn mice (8).

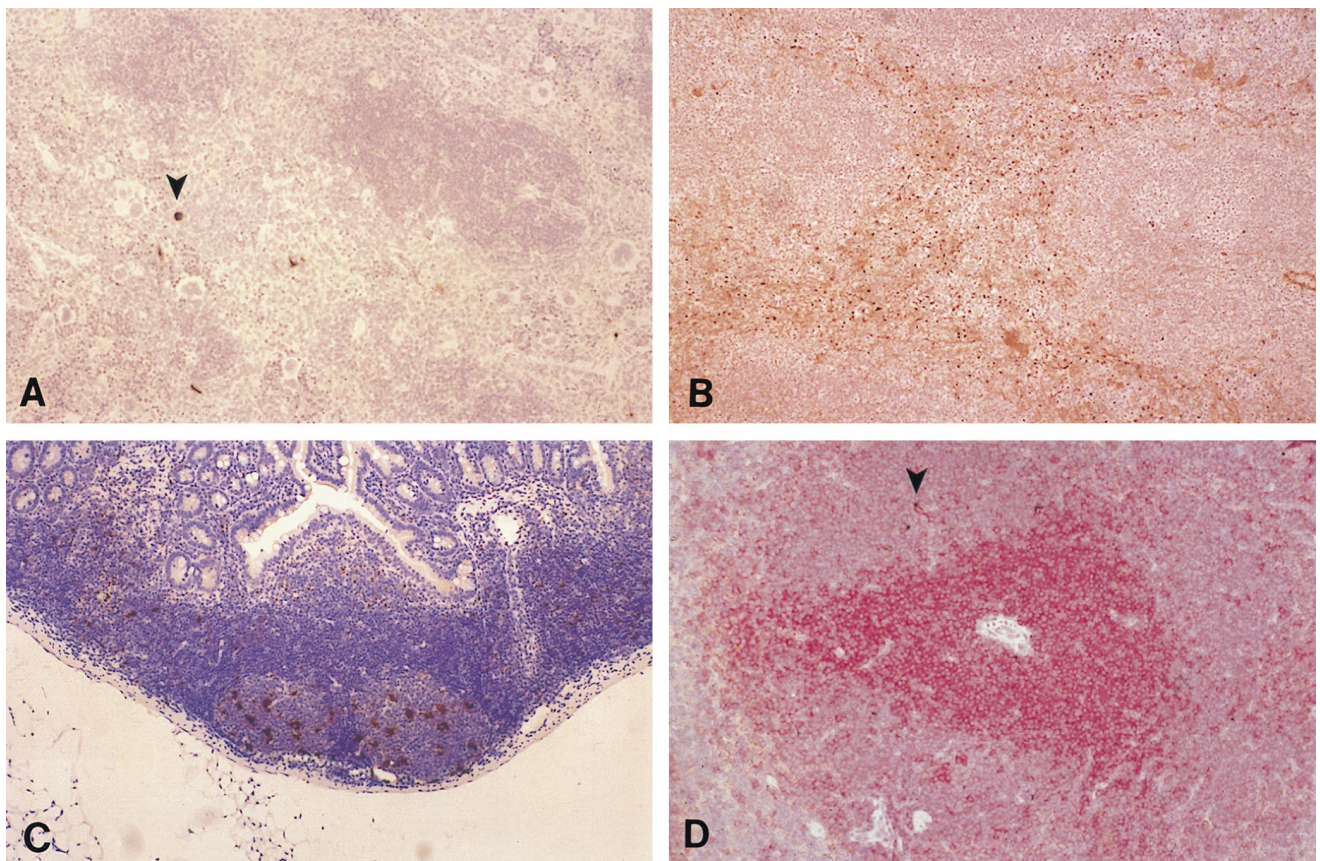


FIG. 4. Infection of lymphoid tissue. (A) In situ hybridization with MAV-1 E3 riboprobe; red pulp of spleen of an i.p.-infected mouse at 7 dpi. The arrowhead indicates positive cells. Magnification,  $\times 48.5$ . (B) Immunohistochemistry with antivirion (AKO-1-68) antiserum; red pulp of an i.p.-infected mouse at 9 dpi. Magnification,  $\times 48.5$ . (C) In situ hybridization with MAV-1 E3 riboprobe; positive stellate-shaped cells in germinal centers of Peyer's patches in an i.p.-infected mouse at 7 dpi. Magnification,  $\times 48.5$ . (D) In situ hybridization with MAV-1 E3 riboprobe plus immunohistochemistry with anti-CD3 antibodies to stain T cells; view of periarteriolar sheath in spleen of an i.n.-infected mouse at 4 dpi. Arrowheads indicate in situ hybridization signals. Positive staining for T cells appears red. Magnification,  $\times 68$ .

TABLE 1. Detection of viral nucleic acids by in situ hybridization in tissues of mice infected by the i.p. or i.n. route

| Route | Organ           | In situ hybridization <sup>a</sup> at indicated dpi |    |                |     |    |                |     |    |    |                |                |                 |
|-------|-----------------|---|----|----------------|-----|----|----------------|-----|----|----|----------------|----------------|-----------------|
|       |                 | 1   | 2  | 3              | 4   | 5  | 7              | 9   | 11 | 13 | 17             |                |                 |
| i.n.  | Spleen          |   |    | +              | +++ |    |                |     |    |    |                | ++             | ND <sup>b</sup> |
|       | Lung            |   |    |                |     |    |                |     |    |    |                | ++             | ND              |
|       | Brain           |   |    |                |     |    |                |     |    |    |                | ++             | ND              |
|       | Spinal cord     |   |    |                |     |    |                |     |    |    |                | ++             | ND              |
|       | Kidney          |   |    |                | +   |    |                |     |    |    |                |                | ND              |
|       | Peyer's patches |   |    |                | +   |    |                |     |    |    |                | +              | ND              |
|       | Lymph node      |   |    | + <sup>c</sup> |     |    |                |     |    |    |                | + <sup>c</sup> | ND              |
| i.p.  | Spleen          |   | ND | +              | ND  |    | +++            | +++ | ++ | ++ | ++             | ++             | ++              |
|       | Lung            |   | ND |                | ND  |    | +++            | +   |    |    |                |                |                 |
|       | Brain           |   | ND |                | ND  |    | +++            | ++  |    |    |                |                |                 |
|       | Spinal cord     | ND  | ND | ND             | ND  | ND | ND             | ND  | ND | ND | ND             | ND             | ND              |
|       | Kidney          |   | ND |                | ND  |    | +              | +   |    |    | +              | +              |                 |
|       | Peyer's patches |   | ND |                | ND  |    | +              | +   |    |    |                |                |                 |
|       | Lymph node      |   | ND |                | ND  |    | + <sup>c</sup> |     |    |    | + <sup>d</sup> |                | + <sup>d</sup>  |

<sup>a</sup> +, viral nucleic acid was presented but very infrequent; ++, few high-power fields had viral nucleic acid; +++, most high-power fields had viral nucleic acid.  
<sup>b</sup> ND, not done.  
<sup>c</sup> Mandibular.  
<sup>d</sup> Prefemoral.

Our results indicate that MAV-1 exhibits a marked endotheliotropism in its natural host and suggest that the recently observed neurologic syndrome (10, 18) is just a manifestation of a wide involvement of the microvascular endothelium. Signs of disease are referable to this primary target of the virus.

Recent reports in the literature have provided examples of other endotheliotropic viruses among the *Adenoviridae*. Bovine adenovirus type 10 (21) has been shown to infect the vascular endothelium of several organs in cases of fatal enteric disease of cattle. Systemic vasculitis with endothelial adenovirus intranuclear inclusions was found in an epizootic of high mortality in the mule deer population of northern California (27). Aggregates of adenovirus particles were detected by electron microscopy in endothelial cells in a case of disseminated adenovirus infection in a domestic cat (16). Canine adenovirus type 1, the cause of infectious canine hepatitis, has a distinct tropism for endothelium and hepatic parenchyma and is excreted in the urine of infected animals for long periods (15). Interestingly, the vascular endothelium has been shown to harbor murine cytomegalovirus in latently infected mice (17).

Replication in lymphoid tissue is also a feature shared by several adenoviruses. Avian hemorrhagic enteritis virus, a type II avian adenovirus, has been shown to replicate in vivo in B lymphocytes and mononuclear phagocytic cells but not in CD4<sup>+</sup> and CD8<sup>+</sup> lymphocytes (22). In addition, there are reports of persistent human adenovirus infection of lymphoid cells in vivo (6, 14, 23). Therefore, the different cell populations shown by this study to harbor virus during the acute disease should be carefully examined with respect to their potential to support a persistent or latent MAV-1 infection.

ACKNOWLEDGMENTS

We thank Amy Ball for preparation of disrupted MAV-1 virions and initial testing of the antiviral antiserum, Gwen Hirsch and Kaija Lewis for technical assistance, and Jai Behari and members of the Spindler lab for comments on the manuscript.

This work was supported by NIH R01 AI23762 and in part by a postdoctoral fellowship from the National Multiple Sclerosis Society to

A.E.K. K.R.S. is the recipient of an NIH Research Career Development Award.

REFERENCES

- Ando, K., L. G. Guidotti, A. Cerny, T. Ishikawa, and F. V. Chisari. 1994. CTL access to tissue antigen is restricted in vivo. *J. Immunol.* **153**:482-488.
- Ball, A. O., M. E. Williams, and K. R. Spindler. 1988. Identification of mouse adenovirus type 1 early region 1: DNA sequence and a conserved transactivating function. *J. Virol.* **62**:3947-3957.
- Beard, C. W., A. O. Ball, E. H. Wooley, and K. R. Spindler. 1990. Transcription mapping of mouse adenovirus type 1 early region 3. *Virology* **175**:81-90.
- Blailock, Z. R., E. R. Rabin, and J. L. Melnick. 1967. Adenovirus endocarditis in mice. *Science* **157**:69-70.
- Blailock, Z. R., E. R. Rabin, and J. L. Melnick. 1968. Adenovirus myocarditis in mice: an electron microscopic study. *Exp. Mol. Pathol.* **9**:84-96.
- Flomenberg, P., V. Piaskowski, J. Harb, A. Segura, and J. T. Casper. 1996. Spontaneous, persistent infection of a B-cell lymphoma with adenovirus. *J. Med. Virol.* **48**:267-272.
- Ginder, D. R. 1964. Increased susceptibility of mice infected with mouse adenovirus to Escherichia coli-induced pyelonephritis. *J. Exp. Med.* **120**:1117-1128.
- Greenlee, J. E., S. H. Clawson, R. C. Phelps, and W. G. Stroop. 1994. Distribution of K-papovavirus in infected newborn mice. *J. Comp. Pathol.* **111**:259-268.
- Greenlee, J. E., R. C. Phelps, and W. G. Stroop. 1991. The major site of murine K papovavirus persistence and reactivation is the renal tubular epithelium. *Microb. Pathog.* **11**:237-247.
- Guida, J. D., G. Fejer, L.-A. Pirofski, C. F. Brosnan, and M. S. Horwitz. 1995. Mouse adenovirus type 1 causes a fatal hemorrhagic encephalomyelitis in adult C57BL/6 but not BALB/c mice. *J. Virol.* **69**:7674-7681.
- Hartley, J. W., and W. P. Rowe. 1960. A new mouse virus apparently related to the adenovirus group. *Virology* **11**:645-647.
- Heck, F. C., Jr., W. G. Sheldon, and C. A. Geisler. 1972. Pathogenesis of experimentally produced mouse adenovirus infection in mice. *Am. J. Vet. Res.* **33**:841-846.
- Hoenig, E. M., G. Margolis, L. Kilham. 1974. Experimental adenovirus infection of the mouse adrenal gland. II. Electron microscopic observations. *Am. J. Pathol.* **75**:375-394.
- Horvath, J., L. Palkonyay, and J. Weber. 1986. Group C adenovirus DNA sequences in human lymphoid cells. *J. Virol.* **59**:189-192.
- Kelly, W. R. 1993. The liver and biliary system, p. 319-406. *In* K. V. F. Jubb, P. C. Kennedy, and N. Palmer (ed.), *Pathology of domestic animals*, 4th ed., vol. 2. Academic Press, San Diego, Calif.
- Kennedy, F. A., and T. P. Mullaney. 1993. Disseminated adenovirus infection in a cat. *J. Vet. Diagn. Invest.* **5**:273-276.
- Koffron, A. J., K. H. Mueller, D. B. Kaufman, F. P. Stuart, B. Patterson, and M. I. Abecassis. 1995. Direct evidence using in situ polymerase chain reaction that the endothelial cell and T-lymphocyte harbor latent murine cytomegalovirus. *Scand. J. Infect. Dis. Suppl.* **99**:61-62.
- Kring, S. C., C. S. King, and K. R. Spindler. 1995. Susceptibility and signs associated with mouse adenovirus type 1 infection of adult outbred Swiss mice. *J. Virol.* **69**:8084-8088.
- Numazaki, Y., S. Shigetani, T. Kumasaka, T. Miyazawa, N. Mamanaka, M. Yano, S. Takai, and N. Ishida. 1968. Acute hemorrhagic cystitis in children: isolation of adenovirus type 11. *N. Engl. J. Med.* **278**:700-704.
- Smith, K., and K. R. Spindler. Pathogenesis and persistence of mouse adenovirus infections. *In* R. Ahmed and I. Chen (ed.), *Persistent viral infections*, in press. John Wiley & Sons, Ltd.
- Smith, K., and K. R. Spindler. Unpublished data.
- Smyth, J. A., M. Benkő, D. A. Moffet, and B. Harrach. 1996. Bovine adenovirus type 10 identified in fatal cases of adenovirus-associated enteric disease in cattle by in situ hybridization. *J. Clin. Microbiol.* **34**:1270-1274.
- Suresh, M., and J. M. Sharma. 1996. Pathogenesis of type II avian adenovirus infection in turkeys: in vivo immune cell tropism and tissue distribution of the virus. *J. Virol.* **70**:30-36.
- van der Veen, J., and M. Lambriex. 1973. Relationship of adenovirus to lymphocytes in naturally infected human tonsils and adenoids. *Infect. Immun.* **7**:604-609.
- van der Veen, J., and A. Mes. 1973. Experimental infection with mouse adenovirus in adult mice. *Arch. Gesamte Virusforsch.* **42**:235-241.
- Wigand, R. 1980. Age and susceptibility of Swiss mice for mouse adenovirus, strain FL. *Arch. Virol.* **64**:349-358.
- Winters, A. L., H. K. Brown, and J. K. Carlson. 1981. Interstitial pneumonia induced by a plaque-type variant of mouse adenovirus. *Proc. Soc. Exp. Biol. Med.* **167**:359-364.
- Woods, L. W., P. K. Swift, B. C. Barr, M. C. Horzinek, R. W. Nordhausen, M. H. Stillian, J. F. Patton, M. N. Oliver, K. R. Jones, and N. J. MacLachlan. 1996. Systemic adenovirus infection associated with high mortality in mule deer (*Odocoileus hemionus*) in California. *Vet. Pathol.* **33**:125-132.